arXiv:1607.03352v1 [cond-mat.mes-hall] 12 Jul 2016

Spin Hall conductance in a Y-shaped junction device in presence of tunable spin-orbit coupling

Sudin Ganguly[1]‡ **and Saurabh Basu**[1]

[1]Indian Institute of Technology Guwhati - Guwahati, Assam-781039, India

E-mail: saurabh@iitg.ernet.in

Abstract. We study spin Hall effect in a three terminal Y-shaped device in presence of tunable spin-orbit (SO) interactions via Landauer-Büttiker formalism. We have evolved a fabrication technique for creating different angular separation between the two arms of the Y-shaped device so as to investigate the effect of angular width on the spin Hall conductance (SHC). A smaller angular separation yields a larger conductance. Also arbitrary orientation of the spin quantization axes yields interesting three dimensional contour maps for the SHC corresponding to different angular separation of the Y-shaped device. The results explicitly show breaking of the spin rotational symmetry. Further a systematic study is carried out to compare and contrast between the different SO terms, such as Rashba and Dresselhaus SO interactions and the interplay of the angular separation therein.

Keywords: Spin Hall effect, Y-shaped device, spin-orbit coupling

‡ Corresponding author: sudin@iitg.ernet.in

1. Introduction

After prediction and detection of the spin Hall effect [1, 2, 3, 4] (SHE), the spin-dependent electronic transport has been a central focus of investigation in mesoscopic physics because of its possible applications to spintronics [5, 6]. Generation of dissipationless spin current [7] is one of the features that is believed to be crucial in this respect. In early attempts, generation of spin-polarized currents were obtained by attaching ferromagnetic metallic contacts to the semiconductors [5, 8]. But, the efficiency of the spin injection from a ferromagnet into a semiconductor is poor because of the conductivity mismatch [9] between the two. This drawback can be overcome by producing spin-polarized current intrinsically. Here comes the role of spin-orbit (SO) interaction. A strong spin-orbit scattering generates spin-polarized electrons intrinsically [10].

In general, two types of spin-orbit coupling terms can be present in semiconductor heterostructures having two dimensional electron systems (2DES). One of them is the Dresselhaus spin-orbit coupling (DSOC) which originates from the inversion asymmetry of the zinc blende type of structures [11] . The other is the Rashba spin-orbit coupling (RSOC) which originates due to the effective electric field originating from the asymmetry of the potential confining the 2DES [12]. The Dresselhaus term is found to be dominant in large band gap materials and the strength can be controlled easily by tunning the quantum well width [13]. On the other hand, the Rashba term is dominant in narrow-gap systems where the strength of the Rashba term can be controlled by external gate voltages [14, 15]. The interplay of both types of spin-orbit coupling on the conductance characteristics of nanostructures has been investigated both theoretically [16, 17, 18, 19] and experimentally [20, 21].

Geometry of the scattering region also plays an important role in order to study effects of spin-polarization in presence of spin-orbit interaction. Four terminal junction devices have been studied where unpolarized charge current is driven through the longitudinal leads attached to a semiconducting region with SO coupling induces a pure spin current at the transverse voltage probes without accompanying any charge current [22, 23]. In particular, three terminal structures such as T-shaped [24], Y-shaped [25, 26, 27, 28] devices have also been studied in presence of spin-orbit interaction. In a three terminal structure, one terminal acts as an input to the device, through which unpolarized charge current is injected into the device. The other two terminals act as outputs through which the spin-polarized currents flow out of the device.

Since a three terminal structure is a suitable candidate for studying the SHE, in this paper, we have studied the behaviour of a special type of three terminal device with Y-shaped structure.Since the angular separation between the arms of the Y-shaped geometry can be relevant for studying SHE, we have considered different angles as shown in Fig.1. Also because the rotational symmetry is broken in spin space in presence of the spin-orbit interaction, the spin quantization axes also play an important role in the context of SHE. Motivated by these, we have studied the effects of the angular variation

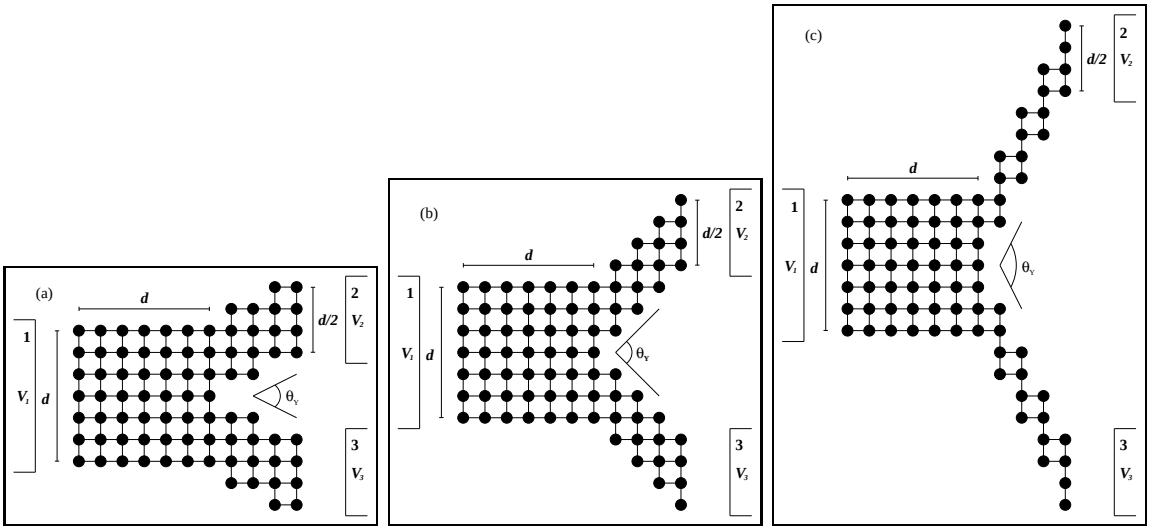

Figure 1. Y-shaped three terminal junction devices with three different angles (θ_Y). V_1, V_2 and V_3 are the applied voltages at the three terminals. The leads are not shown in the figure.

and orientation of the spin quantization axes on the spin Hall conductance of such a Y-shaped junction with tunable SO interactions.

We organize our paper as follows. In the following section, we present a prescription of fabricating a Y-shaped device. The theoretical formalism leading to the expression for the spin Hall conductance using Landauer-Büttiker formula are presented in the next section. After that we include an elaborate discussion of the results obtained for the spin Hall conductance in presence of the SO interaction. We have included an interesting comparison for the conductance properties in presence of Rashba vis-a-vis Dresselhaus SO interactions.

2. Fabrication of Y-shaped devices

We begin our discussion by a prescription of fabricating a Y-shaped junction device which should be interesting from an experimental perspective.

We choose a three-probe measuring set-up as shown in Fig.1 to observe the spin Hall effect. Here the three ideal semi-infinite leads are attached to the central conducting region, which in our case is the Y-shaped device having a square lattice geometry and includes spin orbit interaction. The leads denoted by 1, 2 and 3 are semi-infinite in nature. The voltages applied at the leads are V_1, V_2 and V_3 respectively. The width of the scattering region is d, while the arms has width $d/2$. In this work, we have taken three different Y-shapes by changing the angle between the two arms of the Y, and call it θ_Y as shown in Fig.1.

Fig.2 provides a technique of how one can fix the angle, θ_Y. According to Fig.1, θ_Y is twice the angle as shown in Fig.2. For the Y-shape shown in Fig.1(a), we add the lattice sites in the arms of Y as depicted in Fig.2(a). First we add three sites along x-axis

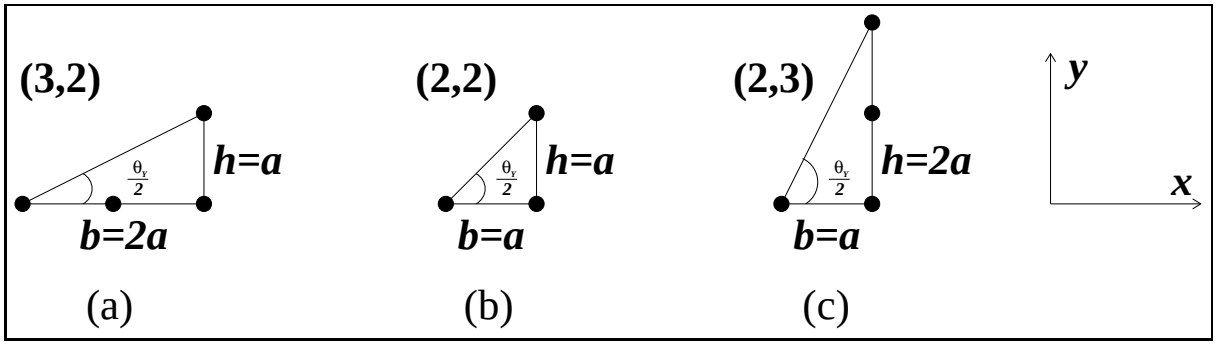

Figure 2. Measurement of the angle between the two arms of the Y-shaped device is shown. b is the base of the triangle and h is the height. a is the lattice constant. According to Fig.1, this angle is half of θ_Y as depicted in the given figure.

with spacing 'a' and then add another site along y-axis just above the third site along x. We repeat the same procedure to build up the rest of the arm of the Y-geometry. Since we need three sites along x-axis and two sites along y-axis we call it a (3,2) scheme. The calculation of the angle in now straight forward from the geometry. From Fig.2, b is the base of the triangle and h is the height. In the (3,2) scheme, $b = 2a$ and $h = a$. Hence, the angular separation between the arms of the Y will be twice the calculated angle and is, $\theta_Y = 2\tan^{-1}\frac{a}{2a} = 53.13°$. Similarly, corresponding to $\theta_Y = 90°$, we need the (2,2) scheme, for which two sites along x-axis and one site along y-axis above the second site along x are required, as shown in Fig.2(b). In the given case, $\theta_Y = 2\tan^{-1}\frac{a}{a} = 90°$. To obtain an angle, θ_Y greater than 90°, we adopt (2,3) scheme as shown in Fig.2(c). Here, $\theta_Y = 2\tan^{-1}\frac{2a}{a} = 128.87°$.

However, we have been able to generate a number of other values for the angular separation, θ_Y by following the prescription given above.

3. Theoretical formulation

3.1. System and Hamiltonian

The single particle Hamiltonian for an electron in presence of both Rashba and Dresselhaus spin-orbit interaction in a two dimensional electron system is given by,

$$H = \frac{\mathbf{p}^2}{2m^*} + \frac{\alpha}{\hbar}\left(\sigma_x p_y - \sigma_y p_x\right) + \frac{\beta}{\hbar}\left(\sigma_x p_x - \sigma_y p_y\right) \tag{1}$$

where $\mathbf{p}$ $(= p_x,\ p_y)$ is the two dimensional momentum operator, m^* is the effective mass, σ_x and σ_y are the components of the Pauli matrices. α and β respective denote the Rashba and Dresselhaus spin-orbit coupling strengths.

We discretize the Hamiltonian via a tight binding approximation with nearest neighbour hopping. The resulting Hamiltonian becomes,

$$H = \epsilon \sum_{i,\sigma} c^\dagger_{i\sigma} c_{i\sigma} + t \sum_{\langle ij\rangle,\sigma} c^\dagger_{i\sigma} c_{j\sigma}$$

$$+V_R \sum_i \left[\left(c^\dagger_{i\uparrow} c_{i+\delta_x\downarrow} - c^\dagger_{i\downarrow} c_{i+\delta_x\uparrow} \right) - i \left(c^\dagger_{i\uparrow} c_{i+\delta_y\downarrow} + c^\dagger_{i\downarrow} c_{i+\delta_y\uparrow} \right) \right]$$
$$+V_D \sum_i \left[(-i) \left(c^\dagger_{i\uparrow} c_{i+\delta_x\downarrow} + c^\dagger_{i\downarrow} c_{i+\delta_x\uparrow} \right) + \left(c^\dagger_{i\uparrow} c_{i+\delta_y\downarrow} - c^\dagger_{i\downarrow} c_{i+\delta_y\uparrow} \right) \right] \quad (2)$$

Here ϵ is the on-site potential and $t = \hbar^2/2m^*a^2$ is the hopping strength, $V_R = \alpha/a$ and $V_D = \beta/a$ are the Rashba and Dresselhaus coupling strengths respectively, a being the lattice constant. $\delta_{x/y}$ is the unit vector along x/y direction.

It is assumed that the Rashba and Dresselhaus SO interactions are present only in the Y-shaped device. The leads are metallic and semi-infinite in nature. The leads are free from any kind of SO interactions so as to avoid any kind or spin flips at the boundaries.

3.2. Formulation spin Hall conductance

Since the rotational symmetry in spin space is lost in presence of spin-orbit interaction, the quantization axes of the spin play a vital role in measuring spin current. Hence we choose the spin quantization axis along an arbitrary direction, say $\hat{\mathbf{u}}$, pointing along (θ, ϕ), where θ and ϕ are the usual spherical angles ($\hat{\mathbf{u}} = \sin\theta\cos\phi, \sin\theta\sin\phi, \cos\theta$).

Now we proceed to evaluate the expression for spin Hall conductance. In order to get pure spin current, we treat terminal 2 as a voltage probe (Fig.1). As a result pure spin current will flow through terminal 2, due to the flow of charge current between terminals 1 and 3. For the three terminal case, the spin Hall conductance is defined as [29],

$$G_{SH} = \frac{\hbar}{2e} \frac{I^s_2}{V_2 - V_1} \quad (3)$$

where I^s_2 is the spin current flowing through lead-2. V_m is the potential at the m-th lead.

The calculation of the electric and spin currents is based on the Landauer-Büttiker multi-probe formalism [30]. The charge and spin currents flowing through lead m ($m = 1, 2, 3$) with potential, V_m can be written in terms of the spin resolved transmission probability as [25],

$$I^q_m = \frac{e^2}{h} \sum_{n \neq m, \sigma, \sigma'} \left(T^{\sigma\sigma'}_{nm} V_m - T^{\sigma'\sigma}_{mn} V_n \right) \quad (4)$$

and,

$$I^s_m = \frac{e^2}{h} \sum_{n \neq m, \sigma'} \left[\left(T^{\sigma'\sigma}_{nm} - T^{\sigma'-\sigma}_{nm} \right) V_m + \left(T^{-\sigma\sigma'}_{mn} - T^{\sigma\sigma'}_{mn} \right) V_n \right]$$
$$= \frac{e^2}{h} \sum_{n \neq m} \left[T^{out}_{nm} V_m - T^{in}_{mn} V_n \right] \quad (5)$$

where, we have defined two useful quantities as follows,

$$\begin{aligned} T_{pq}^{in} &= T_{pq}^{\uparrow\uparrow} + T_{pq}^{\uparrow\downarrow} - T_{pq}^{\downarrow\uparrow} - T_{pq}^{\downarrow\downarrow} \\ T_{pq}^{out} &= T_{pq}^{\uparrow\uparrow} + T_{pq}^{\downarrow\uparrow} - T_{pq}^{\uparrow\downarrow} - T_{pq}^{\downarrow\downarrow} \end{aligned} \tag{6}$$

Physically, the term $\frac{e^2}{h}\sum_{n\neq m} T_{nm}^{out} V_m$ is the total spin current flowing out from the m-th lead with potential V_m to all other n leads, while the term $\frac{e^2}{h}\sum_{n\neq m} T_{mn}^{in} V_n$ is the total spin current flowing into the m-th lead from all other n leads having potential V_n.

The zero temperature conductance, $G_{pq}^{\sigma\sigma'}$ that describes the spin resolved transport measurements, is related to the spin resolved transmission coefficient by [31, 32],

$$G_{pq}^{\sigma\sigma'} = \frac{e^2}{h} T_{pq}^{\sigma\sigma'}(E) \tag{7}$$

The transmission coefficient can be calculated from [33, 34],

$$T_{pq}^{\sigma\sigma'} = \mathrm{Tr}\left[\Gamma_p^{\sigma} G_R \Gamma_q^{\sigma'} G_A\right] \tag{8}$$

Γ_p^{σ}'s are the coupling matrices representing the coupling between the central region and the leads, and they are defined by the relation [35],

$$\Gamma_p^{\sigma} = i\left[\Sigma_p^{\sigma} - (\Sigma_p^{\sigma})^{\dagger}\right] \tag{9}$$

Here Σ_p^{σ} is the retarded self-energy for spin σ associated with the lead p. The self-energy contribution is computed by modeling each terminal as a semi-infinite perfect wire [36].

The retarded Green's function, G_R is computed using

$$G_R = \left(E - H - \sum_{p=1}^{4} \Sigma_p\right)^{-1} \tag{10}$$

where E is the Fermi energy and H is the model Hamiltonian for the central conducting region as given in Eq.(2). G_A is the advanced Green's function and is given by,

$$G_A = G_R^{\dagger} \tag{11}$$

Now, following the spin Hall phenomenology, in our set-up since lead-2 is a voltage probe, $I_2^q = 0$. Also, as the currents in various leads depend only on voltage differences among them, we can set one of the voltages to zero without any loss of generality. Here we set $V_1 = 0$ and $V_3 = 1$. With the help of these conditions, from Eq.(4), one can determine the voltage, V_2,

$$V_2 = \frac{T_{23}}{T_{12} + T_{32}} \tag{12}$$

Further the spin current flowing through terminal 2 (from Eq.(5)) is,

$$I_2^s = \frac{e^2}{h}\left[\left(T_{12}^{\mathrm{out}} + T_{32}^{\mathrm{out}}\right) V_2 - T_{23}^{\mathrm{in}}\right] \tag{13}$$

Finally, from Eq.(3) the expression for the spin Hall conductance is given by,

$$G_{SH} = \frac{e}{4\pi}\left[\left(T_{12}^{\mathrm{out}} + T_{32}^{\mathrm{out}}\right) - T_{23}^{\mathrm{in}} \frac{T_{12} + T_{32}}{T_{23}}\right] \tag{14}$$

4. Results and discussion

We have investigated the effects of the angle variation of the Y-shaped junction in presence of Rashba and Dresselhaus SO couplings on the experimentally measurable quantity, namely the spin Hall conductance (G_{SH}). We have also studied the effect of the orientation of the quantization axis of spin on the spin Hall conductance.

We briefly describe the values of different parameters used in our calculation. Throughout our work, we have considered for the Y-shaped system, $d = 20a$ (see Fig.1), onsite term, $\epsilon = 0$, hopping term, $t = 1$. All the energies are measured in unit of t. Further we choose a unit where $c = h = e = 1$. The spin Hall conductance, G_{SH} is measured in units of $\frac{e}{4\pi}$. Also the lattice constant, a is taken to be unity. For most of our numerical calculations we have used KWANT [37].

From the experimental perspective, we have included a brief discussion on the realistic values of the SO couplings, observed in materials. In GaAs, the effective mass, $m^* = 0.067m_0$ and the lattice constant, $a = 0.5653$ nm. With these values, the hopping integral becomes $t \simeq 1.8$ eV (from the discussion following Eq.(2)). Also in InAlAs/InGaAs it is found that the Rashba parameter is, $\alpha \sim 0.67\times10^{-11}$ eV-m [14, 20]. Then in our case, $V_R = \alpha/a \simeq 0.01$ eV. Since we are denoting all the energy units in terms of t, $V_R/t \simeq 0.006$. Which is pretty small. However, recently, in topological insulators such as Bi_2Se_3, the Rashba coupling parameter is found out to be $\sim 4\times10^{-10}$ eV-m [38], polar semiconductor such as BiTeI shows a bulk Rashba coupling parameter $\sim 3.85 \times 10^{-10}$ eV-m [39]. With these higher values of α, we have $V_R/t \simeq 0.4$, which is of the order of unity and precisely similar in magnitude to what have been used in our work. In fact, we have considered the Rashba and Dresselhaus coupling parameters in the interval $[0 : 1]$.

In this work, we have taken three different angles for the Y-shaped device, such as, θ_Y values to be less than, equal to and greater than 90°. in particular we have considered, $\theta_Y = 53.13^\circ$, 90° and 128.87° as elaborated earlier.

We study the behaviour of the spin Hall conductance as a function of the spin quantization axes parameter, θ and ϕ. In Fig.3, we show the variation of G_{SH} as a function of the spin quantization axes in presence of Rashba SO coupling with strength, $V_R = 0.5$ for three different angles of the Y-shaped device. We set the Fermi energy, to be at $E = -2t$. The nature of G_{SH} for the three plots in Fig.3 are clearly distinct from one another though the RSOC strength is the same. This is because of the difference in the angle, θ_Y, which introduces different scattering environment for the electrons.

In Fig.3(a), G_{SH} shows a symmetric nature along the $\theta = \phi$ line for $\theta_Y = 53.13^\circ$. The color map in Fig.3(a) can be divided into four regions, namely I. ($\theta : 0^\circ - 180^\circ$, $\phi : 0^\circ - 180^\circ$), II. ($\theta : 0^\circ - 180^\circ$, $\phi : 180^\circ - 360^\circ$), III. ($\theta : 180^\circ - 360^\circ$, $\phi : 0^\circ - 180^\circ$) and IV. ($\theta : 180^\circ - 360^\circ$, $\phi : 180^\circ - 360^\circ$). At the center of the each region, G_{SH} has a periodic behaviour (circular patches) which can be seen from the coloured circles. This is raminiscent of the phase space plot for a simple harmonic oscillator. In Fig.3(b), G_{SH} shows different behaviour as a function of θ and ϕ for $\theta_Y = 90^\circ$. For fixed values of ϕ,

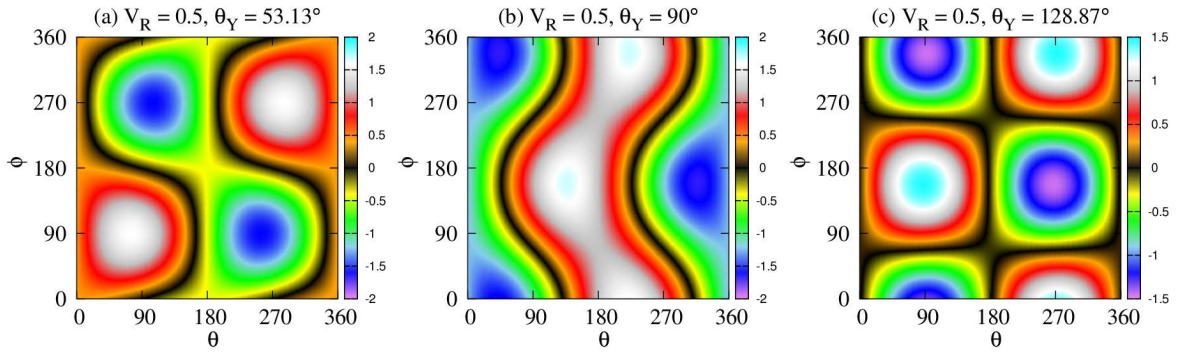

Figure 3. (Color online) Spin Hall conductance, G_{SH} is plotted as a function of the parameters describing the spin quantization axes, namely θ and ϕ for a Fermi energy $E = -2t$ in presence of Rashba spin-orbit coupling with strength, $V_R = 0.5$.

for lower values of θ, G_{SH} starts form negative values. It gradually increases to zero as θ increases. Finally in the vicinity of $\theta = 180°$, G_{SH} becomes positive emphasizing the spin rotational broken symmetry state. For $\theta_Y = 128.87°$, the behaviour of G_{SH} is completely different form the previous two plots as shown in Fig.3(c). Here we get few bounded regions and each region is separated by zero G_{SH} as shown by the dark black line. Along the three lines, namely $\theta = 0°$, $\theta = 180°$ and $\theta = 360°$, the value of G_{SH} is zero. An additional observation is that the magnitude of the spin Hall conductance is lower than the previous two cases.

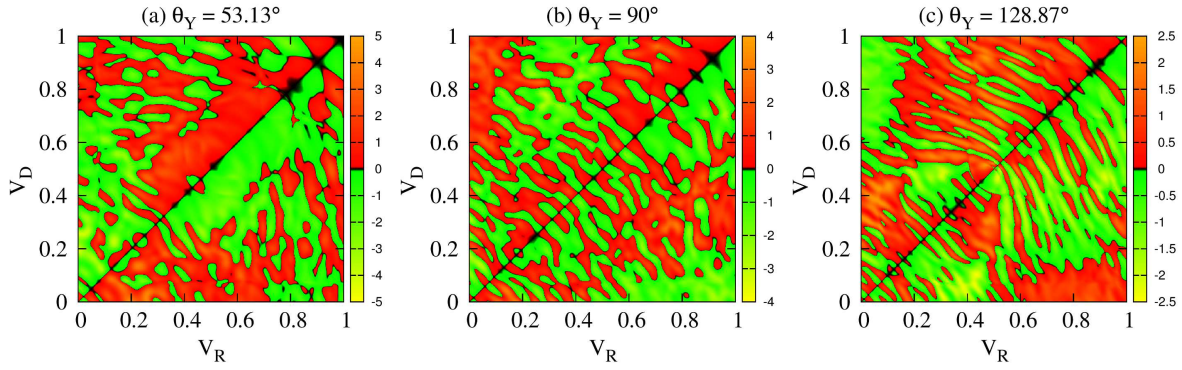

Figure 4. (Color online) Spin Hall conductance, G_{SH} is plotted as a function of the spin-orbit interaction strengths, V_R and V_D for a Fermi energy $E = -2t$. A distinct (and familiar) antisymmetric behaviour is noted.

Let us now study the behaviour of spin Hall conductance as a function of Rashba and Dresselhaus spin-orbit interaction strengths, V_R and V_D respectively. In this case, we set the spin quantization axis along z direction, that is, we fixed (θ, ϕ) to $\theta = 90°$ and $\phi = 0$. Fig.4 shows the variation of G_{SH} as a function of V_R and V_D. Along the $V_R = V_D$ line, G_{SH} is zero, as seen by the black line and the behaviour of G_{SH} is antisymmetric with respect to the $V_R = V_D$ line. It should be noted that this behaviour is expected,

because for $V_R = V_D$, a unitary transformation of the type, $\sigma_x \rightarrow \sigma_y$, $\sigma_y \rightarrow \sigma_x$ and $\sigma_z \rightarrow -\sigma_z$, the Rashba and the Dresselhaus terms get interchanged. By symmetry arguments, the SHC should be zero [18] (also see Fig.5(a)).

For the three different angles, θ_Y, there is an interesting feature if we look at the order of magnitude of G_{SH}. For $\theta_Y = 53.13°$, G_{SH} has the maximum value, while G_{SH} is minimum for $\theta_Y = 128.87°$. This is because different values of θ_Y, causes different scattering environment for the electrons flowing through the leads 2 and 3. In this regard, the positions of the nearest neighbouring sites also play an important role. Since we are measuring the spin current at terminal 2, for a lower θ_Y, electrons reach terminal 2 more easily in comparison to larger values of θ_Y. In other words, the probability of getting scattered towards terminal 2 will be less for larger values of θ_Y. This explains G_{SH} to be small for $\theta_Y = 128.87°$ compared to $\theta_Y = 53.13°$ and $\theta_Y = 90°$.

Motivated by the experiments done on semiconductor quantum wells [40], where the realistic values of the ratio, γ $(= V_R/V_D)$ was discussed to be in the range $\sim 1.5-2.5$, we have studied the variation of G_{SH} as a function of V_R with $V_D = 0$ and vice versa to understand the effects of solely one type of SO interaction.The different parameters are taken as, $E = -2t$, $\theta_Y = 90°$ and the spin quantization is aligned along the z-axis $(\theta = 90°, \phi = 0)$ as shown in Fig.5(a) . There is a nice symmetry (differing by a negative sign) among the behaviour of SHC for the Rashba and Dresselhaus interactions. Also in Fig.5(b), we plot G_{SH} as a function of γ for a fixed V_D, that is, $V_D = 0.5$. For $V_R = V_D$, that is, $\gamma = 1$, $G_{SH} = 0$ as explained earlier. G_{SH} is seen to oscillate about its zero value. The qualitative behaviour of G_{SH} as presented in Fig.5 remains unchanged for a different θ_Y or for other values of the Fermi energy.

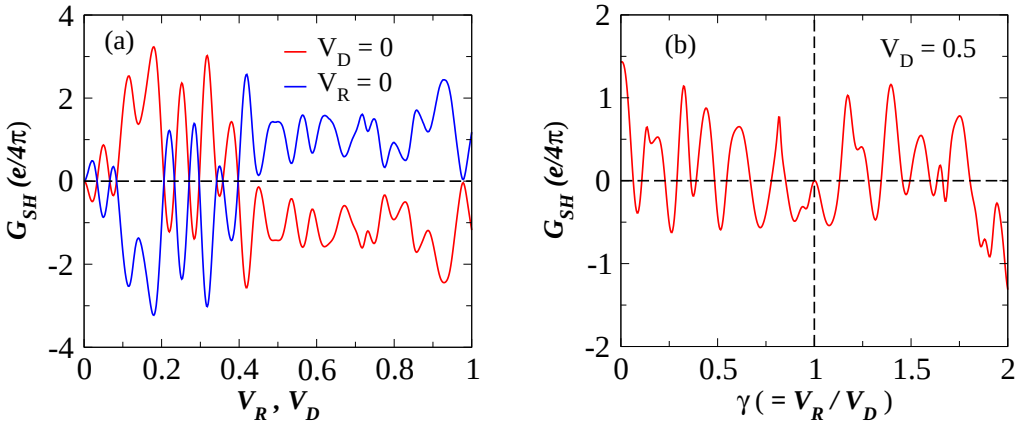

Figure 5. (Color online) (a) Spin Hall conductance, G_{SH} is plotted as a function of V_R (red curve) and V_D (blue curve). (b) G_{SH} is plotted as a function of the ratio, γ $(= V_R/V_D)$. For $\gamma = 0$, G_{SH} is zero. Also the angular separation θ_Y is taken to be 90° here.

5. Summary and Conclusions

In summary, in the present work we have studied the effect of the angular separation of a three terminal Y-shaped junction device in presence of Rashba and Dresselhaus spin orbit couplings on the spin Hall conductance by Landauer-Büttiker formalism. A prescription for the fabrication of the Y-shaped structures with different angular separation is presented. In presence of RSOC, the colour maps of the spin Hall conductance show interesting features as a function of the parameters denoting the spin quantization axes (θ, ϕ) for three different angular separation of the Y-shaped device. A lower angular separation yields a larger G_{SH} owing to enhanced spin Hall current. The results reveal that the rotational symmetry in spin space is lost owing to the SO couplings present therein. A comparison between RSOC and the SO interaction of the other kind, that is, the Dresselhaus SO interaction is made via studying the behaviour of G_{SH}. G_{SH} is antisymmetric in nature with respect to the $V_R = V_D$ line and for $V_R = V_D$, G_{SH} is exactly zero, results that are expected.

We believe that with the advent of improved fabrication technologies, our studies of SHE in three terminal Y-shaped junction devices can be experimentally achievable and should be instrumental in designing newer spintronic devices.

References

[1] M. I. Dyakonov and V. I. Perel, JETP Lett. **13** 467 (1971).
[2] M. I. Dyakonov and V. I. Perel, Phys. Lett. A **35** 459 (1971).
[3] Y. K. Kato, R. C. Myers, A. C. Gossard and D. D. Awschalom, Science **306**, 1910 (2004).
[4] V. Sih, R. C. Myers, Y. K. Kato, W. H. Lau, A. C. Gossard and D. D. Awschalom, Nature Physics **1**, 31 (2005).
[5] S. A. Wolf, D. D. Awschalom, R. A. Buhrman, J. M. Daughton, S. von Molnár, M. L. Roukes, A. Y. Chtchelkanova and D. M. Treger, Science **294**, 1488 (2001).
[6] I. Zutic, J. Fabian, and S. D. Sarma, Rev. Mod. Phys. **76**, 323 (2004).
[7] S. Murakami, N. Nagaosa and S. C. Zhang, Science **301**, 1348 (2003).
[8] S. Datta and B. Das, Appl. Phys. Lett. **56**, 665 (1990).
[9] G. Schmidt, D. Ferrand, L. W. Molenkamp, A. T. Filip, and B. J. van Wees Phys. Rev. B **62**, R4790(R) (2000).
[10] L. D. Landau and E. M. Lifshitz, *Quantum Mechanics: Non-relativistic Theory*, 3rd ed. Pergamon Press, New York, 1991.
[11] G. Dresselhaus, Phys. Rev. **100**, 580 (1955).
[12] E. I. Rashba, Sov. Phys. Solid State **2**, 1109 (1960).
[13] G. Lommer, F. Malcher and U. Rossler, Phys. Rev. Lett. **60**, 728 (1988).
[14] J. Nitta, T. Akazaki, H. Takayanagi and T. Enoki, Phys. Rev. Lett. **78**, 1335 (1997).
[15] G. Engels, J. Lange, Th. Schäpers, and H. Lüth, Phys. Rev. B **55**, R1958 (1997).
[16] E. G. Mishchenko and B.I. Halperin, Phys. Rev. B **68** 045317 (2003).
[17] J. Schliemann and D. Loss, Phys. Rev. B **68** 165311 (2003).
[18] J. Li, L. Hu, S. Q. Shen, Phys. Rev. B **71**, 241305(R) (2005).
[19] C. P. Moca and D. C. Marinescu, Phys. Rev. B **72**, 165335 (2005).
[20] Y. H. Park, H-j Kim, J. Chang, S. H. Han, J. Eom, H-J Choi and H. C. Koo, Appl. Phys. Lett. **103**, 252407 (2013).

[21] A. Sasaki, S. Nonaka, Y. Kunihashi, M. Kohda, T. Bauernfeind, T. Dollinger, K. Richter and J. Nitta, Nature Nanotech. **9**, 703 (2014).
[22] B. K. Nikolić, L. P. Zarbo and S. Souma, Phys. Rev. B **72**, 075361 (2005).
[23] L. Sheng, D. N. Sheng, C. S. Ting, Phys. Rev. Lett. **94**, 016602 (2005).
[24] M. Yamamoto, J. Paaske and P. E. Lindelof, Sceience **299**, 5607 (2003).
[25] T. P. Pareek, Phys. Rev. Lett. **92**, 076601 (2004).
[26] A. W. Cummings, R. Akis and D. K. Ferry, Appl. Phys. Lett. **89**, 172115 (2006).
[27] A. W. Cummings, R. Akis, D. K. Ferry, J. JacobT. Matsuyama, U. Merkt and G. Meier, J. Appl. Phys. **104**, 066106 (2008).
[28] P. Wójcik, J. Adamowski, M.Wołoszyn, and B. J. Spisak, J. Appl. Phys. **118**, 014302 (2015).
[29] M. Dey, S. K. Maiti and S. N. Karmakar, J. Appl. Phys. **112**, 024322 (2012).
[30] M. Büttiker, Phys. Rev. Lett. **57**, 1761 (1986).
[31] R. Landauer, IBM J. Res. Dev. **1**, 223 (1957).
[32] R. Landauer, Philos. Mag. 21, 683 (1970).
[33] C. Caroli, R. Combescot, P. Nozieres and D. Saint-James, J. Phys C: Solid State Phys. **4**, 916, (1971).
[34] D. S. Fisher and P. A. Lee, Phys. Rev. B **23**, 6851 (1981).
[35] S. Dutta, *Electronic transport in Mesoscopic systems*, University press (Cambridge), (1995).
[36] B. K. Nikolić, Phys. Rev. B **64**, 014203 (2001).
[37] C. W. Groth, M. Wimmer, A. R. Akhmerov, X. Waintal, *Kwant: a software package for quantum transport*, New J. Phys. **16**, 063065 (2014).
[38] P. D. C. King, *et al.* Phys. Rev. Lett. **107**, 096802 (2011).
[39] K. Ishizaka, *et al.* Nature Mater. **10**, 521 (2011).
[40] S. D. Ganichev, *et al.* Phys. Rev. Lett. **92**, 256601 (2004) (Also see references therein).